

Lanthanide Metal–Organic Frameworks Showing Luminescence in the Visible and Near-Infrared Regions with Potential for Acetone Sensing

Song Dang,^[a] Xue Min,^[a, b] Weiting Yang,^[a] Fei-Yan Yi,^[a] Hongpeng You,^[a] and Zhong-Ming Sun^{*,[a]}

Abstract: The luminescent properties of a family of lanthanide metal–organic frameworks **LnL** (**Ln** = Y, La–Yb, except Pm; **L** = 4,4'-(2-[(4-carboxyphenoxy)methyl]-2-methylpropane-1,3-diyl)bis(oxy)dibenzoic acid) have been explored, and the energy-transfer process in the compounds has been carefully analyzed. The visible-emitting **Tb_{0.08}Gd_{0.92}L** and the near-infrared (NIR)-luminescent **Yb_{0.10}Gd_{0.90}L** show

excellent optical performances and can be considered as fluorescent probes for acetone sensing based on luminescence quenching effects arising from host–guest interactions. Moreover, **GdL** ex-

hibits a strong second harmonic generation (SHG) signal 6.1 times that of potassium dihydrogen phosphate (KDP) and an outstanding phase-matchable effect. These lanthanide compounds combining fluorescent and nonlinear optical (NLO) properties could meet further requirements as multifunctional materials.

Keywords: lanthanide-based luminescence • metal–organic frameworks • near-infrared luminescence • nonlinear optics • solvent sensing

Introduction


The rational design and construction of lanthanide metal–organic frameworks (LnMOFs) can not only lead to systematically tuned architectures, but also gives rise to multifunctional properties.^[1] LnMOFs with unique optical properties, including large Stokes' shifts, high color purity, and relatively long luminescence lifetimes originating from f–f transitions through the “antenna effect”,^[2] have been emerging as very promising functional materials for sensing applications, such as in the fields of fluorescent probes and luminescence-based bioassays.^[3] Such fluorescent probes appear to be extremely interesting by virtue of their simplicity, rapid response, high sensitivity, and low cost.^[4] The wide variety of luminescent LnMOFs and their inherent synthetic versatility seems to make them ideal for molecular recognition. Molecular recognition mainly relies on interaction between the host material and guest molecules, and this kind of interaction generally depends on the solvent, hydrogen-bonding capability, π – π stacking, and electrostatic interactions.^[5]

LnMOFs with high coordination numbers and various coordination modes of the lanthanide ions can be considered as promising platforms for the recognition of small molecules.^[6] In particular, NIR-luminescent lanthanide materials should prove practically useful because of their versatile applications.^[7] For example, special interest in the Er^{3+} ion for its utility as a planar-wave-guide optical amplifier originates from its 1500 nm emission, which corresponds to one of the standard telecommunication wavelengths.^[8] In vivo luminescent probes based on Yb emission have diagnostic value due to the relative transparency of human tissue at around 1000 nm.^[9] To date, however, only a few examples of NIR-luminescent LnMOFs have been successfully realized for sensing applications.^[10]

Second-order nonlinear optical materials have attracted considerable attention due to their pivotal role in the laser industry, optoelectronic devices, and optical microscopy in biological and medical technologies.^[11,12] Many second-harmonic generation (SHG)-active MOFs have been investigated by rational design of well-defined geometries about the metal centers and highly directional metal–ligand coordination bonds.^[13] Lanthanide complexes have been extensively used for their luminescent, magnetic, and catalytic properties. Investigations of the NLO properties of lanthanides, on the contrary, remain in their infancy and only a few LnMOFs showing NLO responses have been documented.^[14] Consequently, the various applications of NLO materials and the expanding demands for lanthanide materials result in an urgent need for the rational design of lanthanide compounds for second-order NLO applications. One of the most fascinating and significant targets of our research is the preparation of multifunctional materials that combine an

[a] Dr. S. Dang, X. Min, Dr. W. Yang, Dr. F.-Y. Yi, Prof. H. You, Prof. Z.-M. Sun
State Key Laboratory of Rare Earth Resource Utilization
Changchun Institute of Applied Chemistry
Chinese Academy of Sciences
Changchun, 130022 (P. R. China)
E-mail: szm@ciac.ac.cn
Homepage: <http://zhongmingsun.weebly.com>

[b] X. Min
University of Chinese Academy of Sciences
Beijing, 100049 (P. R. China)

 Supporting information for this article is available on the WWW under <http://dx.doi.org/10.1002/chem.201301346>.

ability for molecular recognition with good NLO performance.

Previously, a family of lanthanide metal–organic frameworks, **LnL** (**Ln** = Y, La–Yb, except Pm; **L** = 4,4′-([2-[(4-carboxyphenoxy)methyl]-2-methylpropane-1,3-diyl]bis{oxy})-dibenzoic acid), was synthesized based on a semi-rigid trivalent carboxylic acid.^[15] The compounds all proved to be isostructural and enhanced luminescence properties were elicited by doping Eu, Tb, Dy, and Sm into the Gd analogue; moreover, white-light emissions were successfully achieved. In the work reported herein, we have explored more of the fascinating optical properties of this series of isostructural compounds. The NIR-luminescent properties of the Er and Yb compounds have been studied, and it was found that enhanced NIR luminescence could be obtained by doping. The energy-transfer process in the compounds has been investigated in detail. Furthermore, a Tb-doped compound with excellent optical properties in the visible region and a Yb-doped compound similarly active in the NIR region have been utilized as fluorescent probes for solvent sensing. Good second-order NLO performance of these compounds has also been observed.

Results and Discussion

Structural description: Reaction of **H₃L** and $\text{Ln}(\text{NO}_3)_3 \cdot x\text{H}_2\text{O}$ in *N,N*-dimethylformamide (DMF)/ H_2O (7:1, v/v) at 120 °C afforded plate-like crystals of **LnL** (**Ln** = Y, La–Yb, except Pm). Compounds **LnL** with different lanthanides are all isostructural according to single-crystal X-ray diffraction (XRD) analysis, and crystallize in the orthorhombic space group *Cmc*2₁. The phase purity of the materials was confirmed by powder X-ray diffraction (PXRD) and thermal gravimetric analysis (TGA). Detailed crystallographic information was presented in our previous work.^[15] The Ln^{3+} ions in **LnL** are bridged by organic linkers **L** to form a three-dimensional (3D) framework (Figure 1). One-dimensional channels of about $9.0 \times 9.0 \text{ \AA}^2$ along the *c* axis are

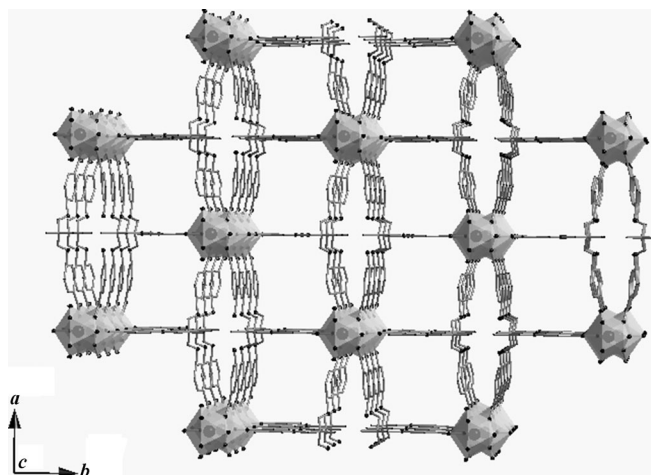


Figure 1. 3D framework structure of **LnL** along the [001] direction.

filled by free DMF molecules. The total potential solvent-accessible void volume is up to 973.4 \AA^3 per unit cell and the pore volume ratio is 31.8% when the guest DMF molecules are removed, calculated with the PLATON program. According to TGA data, the DMF molecules can be easily removed from the pores, leaving the 3D framework intact.

Luminescence properties: Doping has been widely used in the synthesis of new lanthanide materials. It is an effective strategy for enhancing lanthanide-based luminescence.^[16] Since the whole family compounds are isostructural, enhanced performance could be achieved by doping the Gd analogue with Er^{3+} or Yb^{3+} ions. In order to explore the NIR luminescence behavior of the series, a variety of partially substituted Gd compounds were synthesized, denoted as **Ln_xGd_{1-x}L**, in which **Ln** = Er, Yb, and $0 \leq x \leq 1$. The luminescence lifetimes (τ) of the Ln^{3+} ions in the doped materials are given in Tables 1 and 2. The excitation spectra of

Table 1. Luminescence lifetimes (τ) for the $^4\text{I}_{13/2} \rightarrow ^4\text{I}_{15/2}$ transition (1539 nm) of **Er_xGd_{1-x}L**.

<i>x</i>	τ [μs]	<i>x</i>	τ [μs]
0.01	1.01	0.2	2.30
0.02	1.45	0.4	2.31
0.04	1.49	0.8	1.52
0.08	3.01	1	1.43

Table 2. Luminescence lifetimes (τ) for the $^2\text{F}_{5/2} \rightarrow ^2\text{F}_{7/2}$ transition (983 nm) of **Yb_xGd_{1-x}L**.

<i>x</i>	τ [μs]	<i>x</i>	τ [μs]
0.005	9.23	0.1	33.46
0.01	18.91	0.2	25.50
0.02	24.10	0.4	9.10
0.04	26.88	1	1.82

ErL and **YbL** are shown in Figures S1 and S2, respectively. The excitation bands at around 290 nm are ascribed to the absorption of **H₃L**. The emission spectra of Er-doped compounds, excited at 290 nm, are shown in Figure 2a. The characteristic emission of the Er^{3+} ion at 1539 nm can be seen, which can be attributed to its $^4\text{I}_{13/2} \rightarrow ^4\text{I}_{15/2}$ transition. Compared to those of **ErL**, the emission intensity and the emission lifetime of **Er_{0.08}Gd_{0.92}L** were increased 2.7-fold and 2.1-fold, respectively, the latter from 1.43 to 3.01 μs . Figure 2b shows the emission spectra of the series of Yb-doped compounds. A prominent emission band can be observed at 983 nm, attributable to the $^2\text{F}_{5/2} \rightarrow ^2\text{F}_{7/2}$ transition of the Yb^{3+} ion. Compared with those of **YbL**, the emission intensity of the peak at 983 nm and the emission lifetime of **Yb_{0.10}Gd_{0.90}L** were increased 10.5- and 18.4-fold, respectively, the latter from 1.82 to 33.46 μs . The absence of the ligand emission implies an efficient energy transfer from the ligand to the Ln^{3+} ions.

It is known that lanthanide complexes can be effectively sensitized by organic ligands through the so-called “antenna

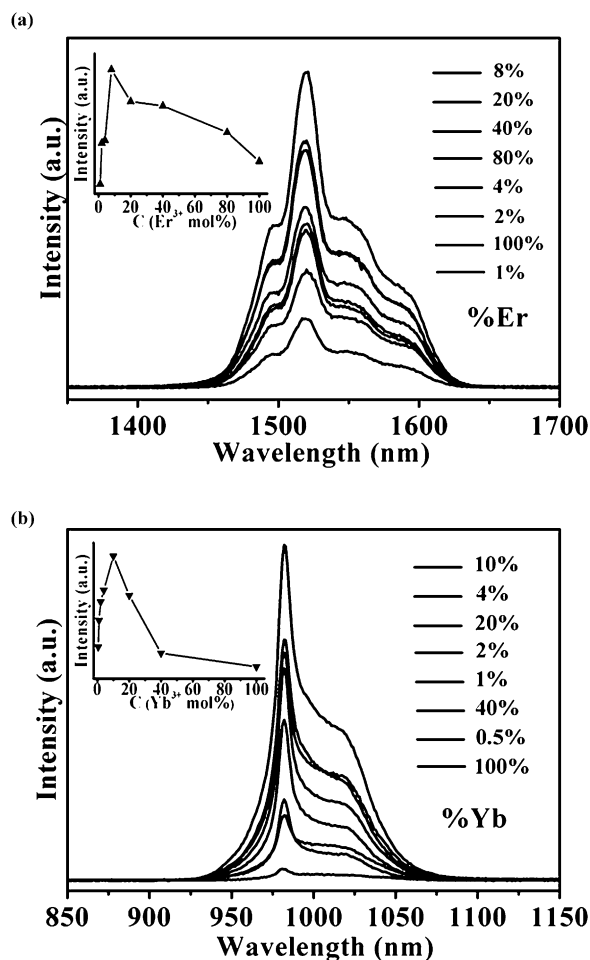


Figure 2. Emission spectra of a) $\text{Er}_x\text{Gd}_{1-x}\text{L}$ and b) $\text{Yb}_x\text{Gd}_{1-x}\text{L}$ solid samples, $\lambda_{\text{ex}}=290$ nm. The inset figures indicate the corresponding transition intensities of the doped compounds as a function of doping concentration x .

effect". Based on fluorescence measurements, it is believed that the luminescence of Ln^{3+} ions ($\text{Ln}=\text{Eu}, \text{Tb}, \text{Dy}, \text{Sm}, \text{Er},$ and Yb) can be sensitized by energy transfer from the triplet excited states of **L**. On this basis, a model is proposed to describe the indirect excitation process (see Figure 3). The ligands firstly absorb energy and are excited from the singlet S_0 ground state to the singlet S_1 excited state. The energy is then transferred to the triplet excited state of the ligands by intersystem crossing, and this is followed by relaxation from the upper 4f levels to the first excited states of the Ln^{3+} ions, resulting in the emission of the sensitized Ln^{3+} ions. According to Dexter's theory, the suitability of the energy gap between an Ln^{3+} ion and the ligand is crucial for efficient energy transfer.^[17] If the energy gap is too wide, the energy-transfer rate constant will decrease due to diminution in the overlap between the donor (ligand) and the acceptor (Ln^{3+} ion). In contrast, if the energy gap is too narrow, there will be energy back-transfer from the Ln^{3+} ion to the resonance level of the triplet state of the ligand. The triplet-state (T_1) energy level of **L** is $22\,600\text{ cm}^{-1}$, calculated from the phosphorescence spectrum of the Gd^{III} com-

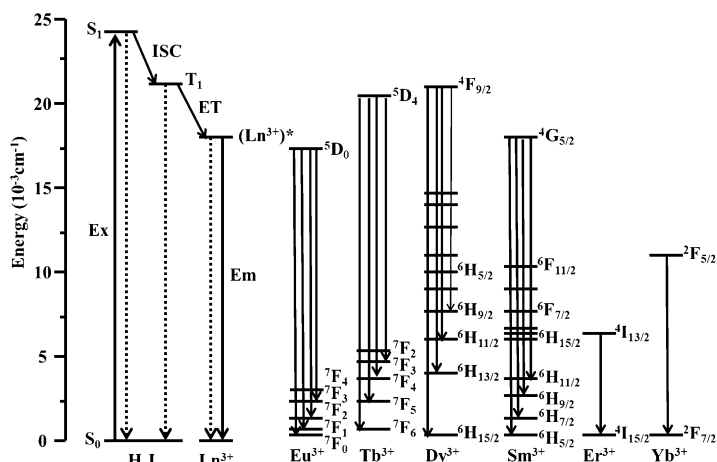


Figure 3. Left: Model for the main intramolecular energy-transfer process. Right: energy diagram of the 4f levels of the Ln^{3+} ions ($\text{Ln}=\text{Eu}, \text{Tb}, \text{Dy}, \text{Sm}, \text{Er},$ and Yb).

plex measured at 77 K upon excitation at 290 nm (Figure S3). The T_1 energy level of **L** is thus 5300 cm^{-1} higher than the $^5\text{D}_0$ level of Eu^{III} ($17\,300\text{ cm}^{-1}$), 2100 cm^{-1} higher than the $^5\text{D}_4$ level of Tb^{III} ($20\,500\text{ cm}^{-1}$), 1600 cm^{-1} higher than the $^4\text{F}_{9/2}$ level of Dy^{III} ($21\,000\text{ cm}^{-1}$), 4700 cm^{-1} higher than the $^4\text{G}_{5/2}$ level of Sm^{III} ($17\,900\text{ cm}^{-1}$), $16\,000\text{ cm}^{-1}$ higher than the $^4\text{I}_{13/2}$ level of Er^{III} (6600 cm^{-1}), and $12\,300\text{ cm}^{-1}$ higher than the $^2\text{F}_{5/2}$ level of Yb^{III} ($10\,300\text{ cm}^{-1}$). According to the luminescence theory of lanthanide complexes, the ligand **L** can clearly sensitize the luminescence of the Ln^{3+} ions, and the energy transfer from the ligand to the Ln^{3+} ions follows the sequence $\text{Tb}^{3+} > \text{Eu}^{3+}, \text{Dy}^{3+}, \text{Sm}^{3+} > \text{Er}^{3+}, \text{Yb}^{3+}$.^[18] This phenomenon is consistent with the results of the PL measurements. **TbL** displays excellent luminescence behavior, including the luminescence intensity and quantum yield. The weaker PL intensities of the Eu and Sm complexes may be attributed to the large energy differences between the ligand and the Ln^{3+} ions; on the contrary, the small energy gap between **L** and the Dy^{3+} ion may lead to an energy back-transfer process. Therefore, in the case of $\text{Eu}^{3+}, \text{Dy}^{3+},$ and Sm^{3+} ions, the less efficient energy transfer from the ligand to the Ln^{3+} ions results in weaker luminescence compared to that of the Tb^{3+} ion. Meanwhile, the energy levels of the NIR-luminescent lanthanide ions are much lower than those of the Ln^{3+} ions in the visible region. In our experiments, the Er and Yb complexes showed much weaker luminescence compared to the visible-region-active $\text{Eu}^{3+}, \text{Tb}^{3+}, \text{Dy}^{3+},$ and Sm^{3+} ions, which is the result of less efficient energy transfer considering their much lower energy levels. It is worth noting that Yb complexes exhibit better emission intensity than that of Er complexes, because the energy gap between **L** and the Yb^{3+} ion is smaller. In addition to the ligand-to-metal energy-transfer ability, another benefit of the organic ligand is to saturate the first coordination sphere of the lanthanide ion, thereby effectively protecting the central lanthanide ion from water molecules, which may significantly quench the luminescence.

Solvent sensing: Based on the above discussion, it is evident that $\text{Tb}_{0.08}\text{Gd}_{0.92}\text{L}$ and $\text{Yb}_{0.10}\text{Gd}_{0.90}\text{L}$ possess excellent luminescent properties in the visible and NIR regions, respectively. They have therefore been employed for sensing measurements. Activated compounds $\text{Tb}_{0.08}\text{Gd}_{0.92}\text{L}$ and $\text{Yb}_{0.10}\text{Gd}_{0.90}\text{L}$ were prepared by thermal activation of the corresponding compounds $\text{Ln}_x\text{Gd}_{1-x}\text{L}$ ($\text{Ln} = \text{Tb}, \text{Yb}$) at 140°C in vacuo overnight. To examine the potential applications of $\text{Tb}_{0.08}\text{Gd}_{0.92}\text{L}$ and $\text{Yb}_{0.10}\text{Gd}_{0.90}\text{L}$ in solvent sensing, the respective samples were immersed in various pure solvents for three days to form stable emulsions prior to fluorescence studies. The solvents examined were DMF (*N,N*-dimethylformamide), methanol, ethanol, acetone, 1-propanol, 2-propanol, phenylmethanol, acetonitrile, THF (tetrahydrofuran), toluene, chloroform, and H_2O .

The luminescence properties of $\text{Tb}_{0.08}\text{Gd}_{0.92}\text{L}$ in the various solvents were recorded and compared. As shown in Figure 4, the characteristic emissions of the Tb^{3+} ion were observed in most of the solvents, except for acetone. Evidently, the luminescence intensities of $\text{Tb}_{0.08}\text{Gd}_{0.92}\text{L}$ strongly depend on the solvent molecules, particularly acetone, which exerted the most significant quenching effect. Further

detailed experiments were undertaken to examine the ability of $\text{Tb}_{0.08}\text{Gd}_{0.92}\text{L}$ to sense acetone. Compound $\text{Tb}_{0.08}\text{Gd}_{0.92}\text{L}$ dispersed in 2-propanol was considered as the standard emulsion, and the content of acetone was gradually increased to investigate the emission response. It was found that the luminescence intensity of the compound emulsion gradually decreased with the addition of acetone, as shown in Figure 5. The luminescence of the emulsion was almost undetectable when the acetone content reached 3% (v/v). The decrease in the fluorescence intensity of the $^5\text{D}_4 \rightarrow ^7\text{F}_5$ transition at 544 nm of the Tb^{3+} ion versus the acetone content was well fitted by a first-order exponential decay (Figure 6), implying a diffusion-controlled process for the acetone quenching behavior.^[19]

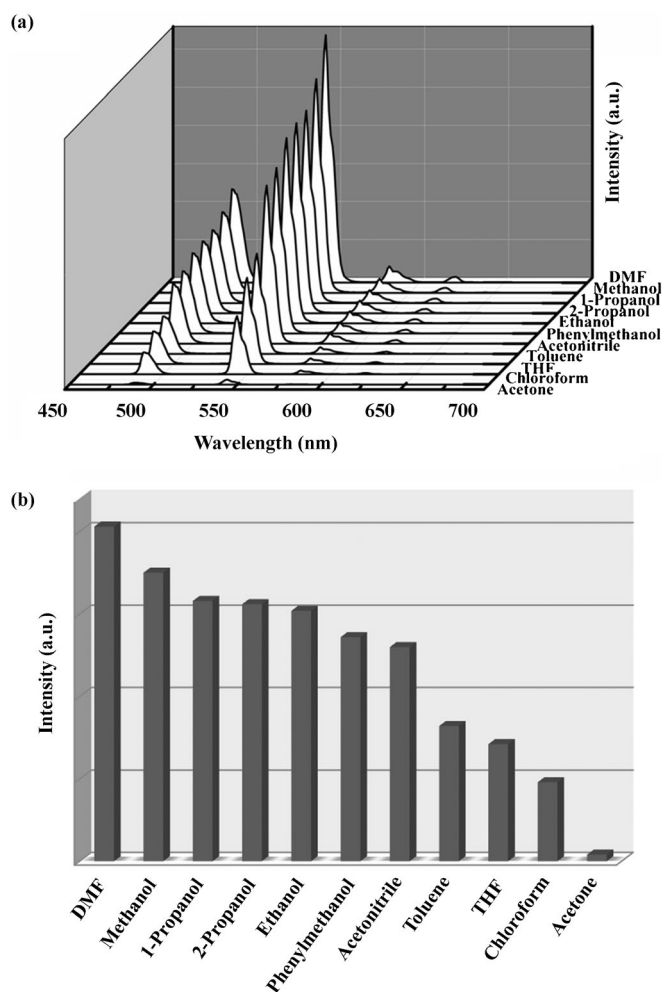


Figure 4. a) Spectra and b) the $^5\text{D}_4 \rightarrow ^7\text{F}_5$ transition (544 nm) intensities of $\text{Tb}_{0.08}\text{Gd}_{0.92}\text{L}$ in various pure solvents, $\lambda_{\text{ex}} = 290$ nm.

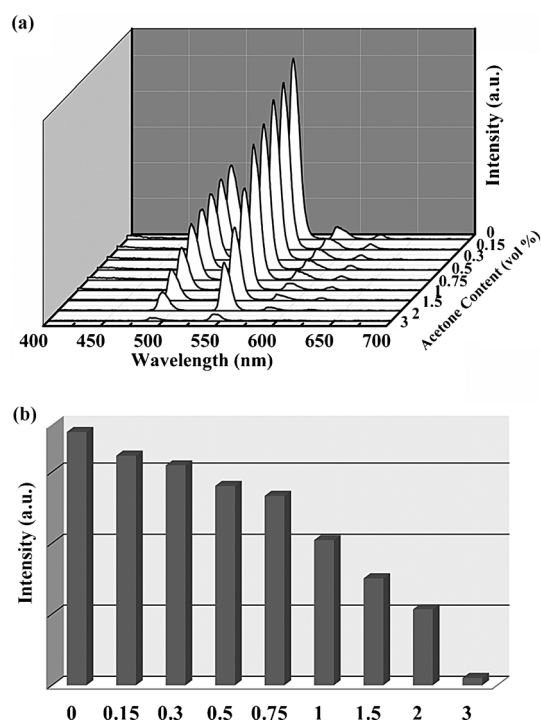


Figure 5. a) Spectra and b) the $^5\text{D}_4 \rightarrow ^7\text{F}_5$ transition (544 nm) intensities of $\text{Tb}_{0.08}\text{Gd}_{0.92}\text{L}/2\text{-propanol}$ emulsion in the presence of different amounts of acetone, $\lambda_{\text{ex}} = 290$ nm.

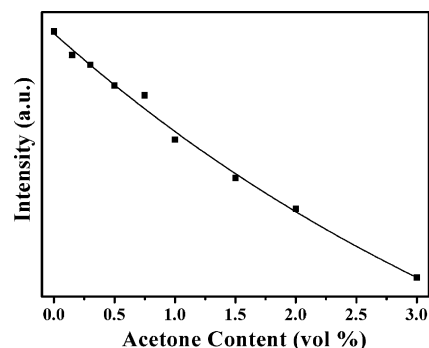


Figure 6. The emission intensity of the $^5\text{D}_4 \rightarrow ^7\text{F}_5$ transition at 544 nm of the Tb^{3+} ion for $\text{Tb}_{0.08}\text{Gd}_{0.92}\text{L}/2\text{-propanol}$ emulsion as a function of acetone content.

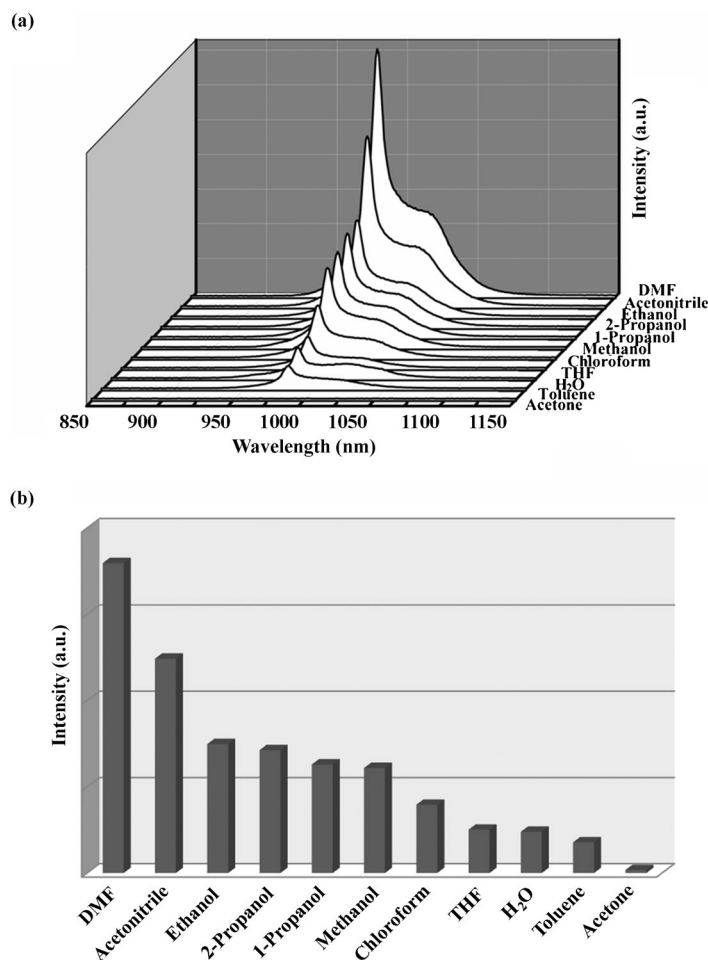


Figure 7. a) Spectra and b) the $^2F_{5/2} \rightarrow ^2F_{7/2}$ transition (983 nm) intensities of $\text{Yb}_{0.10}\text{Gd}_{0.90}\text{L}$ in various pure solvents, $\lambda_{\text{ex}} = 290$ nm.

The influences of various solvents on the fluorescence intensity of NIR-luminescent $\text{Yb}_{0.10}\text{Gd}_{0.90}\text{L}$ were also investigated, as shown in Figure 7. The most intriguing feature was that the PL spectra were also dependent on the solvents, especially acetone, which exerted a significant quenching effect on the Yb luminescence. Moreover, by taking a $\text{Yb}_{0.10}\text{Gd}_{0.90}\text{L}/2$ -propanol emulsion as a standard, addition of acetone resulted in a significant weakening of the luminescence intensity, which almost disappeared at an acetone content of 2.5 vol % (Figure 8). The decrease in the luminescence intensity of the 983 nm emission of the Yb^{3+} ion versus the volume ratio of acetone could be fitted by a single-exponential function (Figure 9), indicating that the luminescence quenching of $\text{Yb}_{0.10}\text{Gd}_{0.90}\text{L}$ by acetone was also diffusion-controlled.^[19]

The luminescence properties of $\text{Tb}_{0.08}\text{Gd}_{0.92}\text{L}$ and $\text{Yb}_{0.10}\text{Gd}_{0.90}\text{L}$ in various solvents were further explored by luminescence lifetime studies of the Ln^{3+} ions ($\text{Ln} = \text{Tb}, \text{Yb}$), and the results are listed in Table 3. The luminescence lifetimes of the compounds were highest in DMF, whereas they were undetectable in acetone. This observation of the lifetimes is in good agreement with the emission spectra.

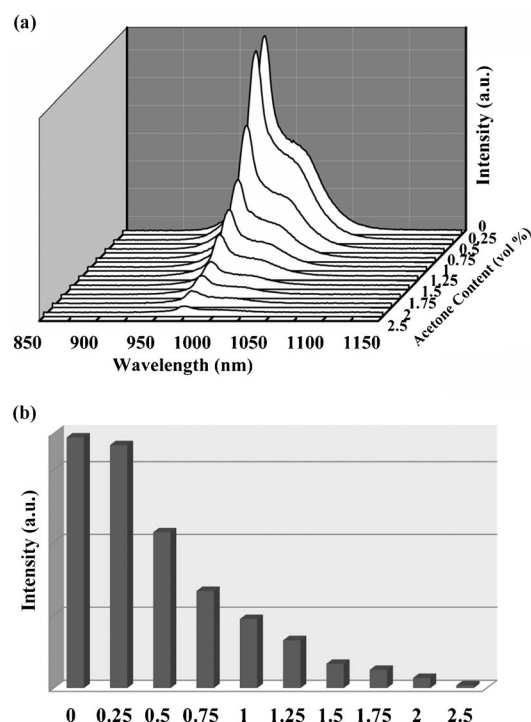


Figure 8. a) Spectra and b) the $^2F_{5/2} \rightarrow ^2F_{7/2}$ transition (983 nm) intensities of $\text{Yb}_{0.10}\text{Gd}_{0.90}\text{L}/2$ -propanol emulsion in the presence of different amounts of acetone, $\lambda_{\text{ex}} = 290$ nm.

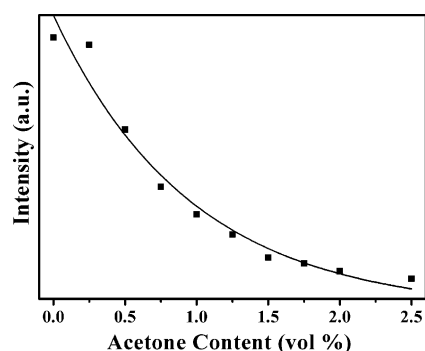


Figure 9. The emission intensity of the $^2F_{5/2} \rightarrow ^2F_{7/2}$ transition of the Yb^{3+} ion at 983 nm for $\text{Yb}_{0.10}\text{Gd}_{0.90}\text{L}/2$ -propanol emulsion as a function of acetone content.

Powder XRD analysis was employed to study the structures of the compounds infused with various solvents, and the obtained patterns are shown in Figures 10 and 11. It is clear that the basic frameworks of the compounds remain intact after introducing the solvent molecules. To investigate the mechanism of the quenching effect, UV absorption spectra of the ligand H_3L were measured in various solvents (Figures S6 and S7). As shown in Figure S6, a broad absorption band ranging from 250 to 300 nm was observed. Acetone exhibits a wider absorption band from 230 to 325 nm (Figure S7), which covers the whole range of that of the ligand H_3L . This means that in an emulsion the acetone will absorb most of the excitation energy and only a small fraction of

Table 3. Luminescence lifetimes for the $^5D_4 \rightarrow ^7F_5$ transition (544 nm) of **Tb**_{0.08}**Gd**_{0.92}**L** and the $^2F_{5/2} \rightarrow ^2F_{7/2}$ transition (983 nm) of **Yb**_{0.10}**Gd**_{0.90}**L** in various solvents.

	DMF	MeOH	1-Prop- anol	2-Prop- anol	EtOH	Aceto- nitrile
Tb _{0.08} Gd _{0.92} L [ms]	0.51	0.46	0.44	0.42	0.44	0.39
Yb _{0.10} Gd _{0.90} L [μs]	12.07	5.30	5.22	5.66	5.44	7.94
	PhCH ₂ OH	Toluene	THF	CHCl ₃	H ₂ O	Acetone
Tb _{0.08} Gd _{0.92} L [ms]	0.37	0.23	0.24	0.16	–	UD ^[a]
Yb _{0.10} Gd _{0.90} L [μs]	–	2.45	2.87	4.41	2.90	UD ^[a]

[a] UD: very weak, undetectable.

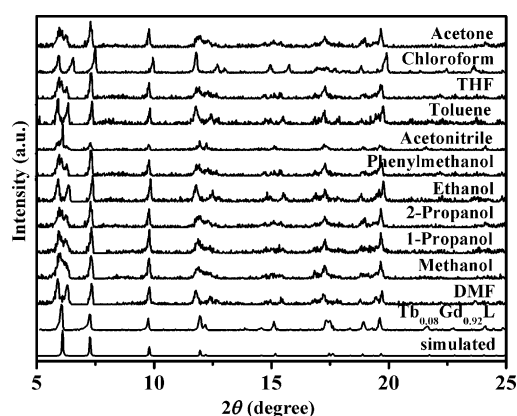


Figure 10. Powder XRD patterns of **Tb**_{0.08}**Gd**_{0.92}**L** infused with various solvents.

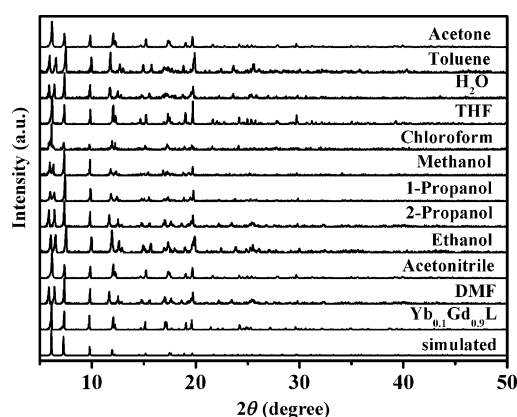


Figure 11. Powder XRD patterns of **Yb**_{0.10}**Gd**_{0.90}**L** infused with various solvents.

the energy will be absorbed by the ligand. Hence, very little energy will be transferred through the ligand to the Ln³⁺ ions. This also explains why toluene and phenylmethanol have lower quenching effects on the samples. These solvents display similar absorption bands in the range 230–275 nm, partly overlapping with that of the ligand (the blue and red lines in Figure S8). In these cases, there will be a competition for the excitation energy between the organic ligands and

the solvent molecules. It is well known that the luminescence of lanthanide compounds mainly relies on sensitization by organic ligands; the solvent molecules could thus influence the energy absorbed by the ligands, resulting in changes in the emissions of the compounds. According to the above discussion, the energy absorbed by the ligand decreases due to solute–solvent interactions between **L** and the acetone molecules, leading to a decreased or even fully quenched lanthanide luminescence. Therefore, **Tb**_{0.08}**Gd**_{0.92}**L** and **Yb**_{0.10}**Gd**_{0.90}**L** can be used as fluorescent probes for acetone sensing. Further experiments were also performed on the quenching of Tb and Yb samples with various other ketones, namely acetophenone, benzophenone, and cyclohexanone (Figures S8–S10). All of these ketones exerted a strong quenching effect on both the Tb and Yb compounds (Figures S9 and S10). Again, this can be rationalized in terms of spectral overlap, referring to the UV absorption spectra of the various ketones in *n*-hexane (Figure S8).

A sensor for solvent vapors would undoubtedly have more practical relevance than one applicable to liquid mixtures of isopropanol/acetone.^[6c] Therefore, we performed additional vapor sensing experiments using the Tb material. The experimental set-up is depicted in Figure S11. It seems that in acetone vapor, however, the material does not exhibit such a strong quenching effect as that in liquid media. The PL intensity decreased to 65% when the solid sample was exposed to acetone vapor for 12 h and there were no significant further changes when the experiment was continued for 1 or 2 days (Figure S12). More experiments will be performed on gas-phase detection in our future work.

Second-order NLO properties: The noncentrosymmetric structure of the isostructural compounds, *Cmc*2₁, prompted us to measure their second harmonic generation (SHG) properties. Taking **GdL** as an example, Kurtz powder SHG measurements were made to confirm its acentricity as well as to evaluate its potential as a second-order NLO material.^[20] The results revealed that **GdL** displays strong SHG efficiency, approximately 6.1 times higher than that of the technologically useful potassium dihydrogen phosphate (KDP) at the same particle size of 150–210 μm (Figure 12a). Moreover, measurements made on **GdL** crystals of various sizes revealed that the SHG intensities increased with increasing particle size and reached a maximum saturation value, implying type I phase-matchable behavior (Figure 12b). It is widely accepted that ideal SHG materials require compounds with high SHG coefficient and phase matchability. Moreover, **GdL** is insoluble in water and most common organic solvents, and is air-stable up to 600 K. All of the above attributes make **GdL** an attractive candidate for use as a second-order NLO material. To the best of our knowledge, only a few examples of three-dimensional structural EuMOFs with such a strong SHG response have hitherto been reported.^[14c] It is hoped that this investigation will encourage more studies devoted to SHG-active LnMOF materials.

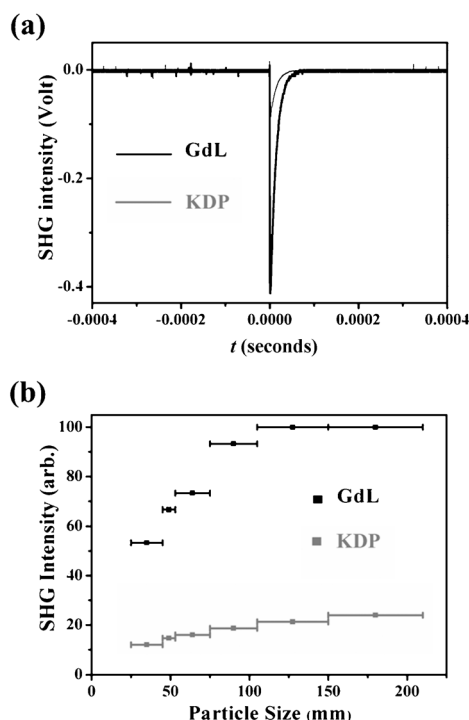


Figure 12. a) Oscilloscope traces of the SHG signals of **GdL** and **KDP** at the same particle size of 150–210 μm . b) Particle-size dependences of the SHG intensity for **GdL** and **KDP**.

Conclusion

In summary, the NIR-luminescent properties of an isostructural family of LnMOFs (**LnL**; **Ln** = Y, La–Yb, except Pm) have been explored and enhanced luminescence has been achieved by doping the Gd compound with Er or Yb. Energy transfer in the luminescent compounds (Eu-, Tb-, Dy-, Sm-, Er-, and Yb-doped) has been evaluated, and it was found that the Tb compound showed excellent luminescence performance and the most efficient energy-transfer process from **L** to the Tb^{3+} ion. Visible-emitting **Tb_{0.08}Gd_{0.92}L** and efficiently NIR-luminescent **Yb_{0.10}Gd_{0.90}L** have been employed as fluorescent probes for solvent sensing. These compounds exhibited significant sensing abilities for acetone based on complete quenching of their luminescence. This can be mainly attributed to less energy being absorbed by the ligand as a result of interactions between the host framework and the guest acetone molecules. Furthermore, **GdL** represents a rare example of an NLO-active material with a strong SHG efficiency (6.1 times that of **KDP**). Multifunctional lanthanide complexes that combine acetone sensing with NLO properties have been realized, which could potentially broaden the applications of such materials. More research work will be devoted to such multifunctional lanthanide materials to meet the different needs of actual applications.

Experimental Section

Instrumentation: Elemental analyses of C, H, and N in the solid samples were performed with a Vario EL analyzer. Thermogravimetric analysis (TGA) was performed using an SDT 2960 simultaneous DSC-TGA from TA Instruments, heating to 800 °C at a rate of 10 °C min⁻¹ under an air flow of 100 mL min⁻¹. Powder X-ray diffraction (XRD) patterns were obtained on a Bruker D8 Focus diffractometer with $\text{CuK}\alpha$ radiation ($\lambda = 0.15405$ nm, continuous, 40 kV, 40 mA, increment = 0.02°). The powder frequency-doubling effect was measured by the method of Kurtz and Perry. The fundamental wavelength of 1064 nm was generated by a Q-switched Nd:YAG laser. The SHG wavelength was thus 532 nm. KH_2PO_4 (**KDP**) was used as a reference. Fluorescence spectra were measured on a Horiba Jobin Yvon Fluorolog-3 fluorescence spectrophotometer, equipped with a 450 W Xe lamp as the excitation source, an iHR320 monochromator, and a liquid-nitrogen-cooled R5509–72 photomultiplier tube (PMT) as detector. Time-resolved measurements were performed using the third harmonic (355 nm) of a Spectra-Physics Nd:YAG laser with a pulse width of 5 ns and an energy per pulse of 5 mJ as the source; the NIR emission lines were dispersed by a Horiba Jobin Yvon iHR320 emission monochromator equipped with a liquid-nitrogen-cooled R5509–72 PMT, and the data were analyzed with a LeCroy WaveRunner 6100 1 GHz oscilloscope. Luminescence lifetimes were calculated with the Origin 7.5 software package. The low-temperature phosphorescence spectrum of **GdL** was measured on a Hitachi F-4500 spectrophotometer at liquid-nitrogen temperature (77 K). The PMT voltage was 700 V, the scan speed was 1200 nm min⁻¹, and the slit width for excitation and emission was 2.5 nm. The strongest emission wavelengths were located at 611 nm following excitation at 290 nm. The mass of each solid sample used for luminescence tests was 40 ± 2 mg.

Synthesis of compounds LnL (Ln** = Y, La–Yb, except Pm):** According to our previous work,^[15] a solution of $\text{Ln}(\text{NO}_3)_3 \cdot 6\text{H}_2\text{O}$ (45 mg, 0.1 mmol) and **H₃L** (48.2 mg, 0.1 mmol) in DMF/ H_2O (8 mL; 7:1, v/v) was placed in a Teflon-lined stainless steel autoclave (20 mL) and heated at 120 °C for 72 h to form the desired crystals. A similar procedure was employed to synthesize **Ln_xGd_{1-x}L** (**Ln** = Er, Yb, $0 \leq x \leq 1$) by adding the appropriate lanthanide nitrates in the required stoichiometry. To obtain activated **Tb_{0.08}Gd_{0.92}L** and **Yb_{0.10}Gd_{0.90}L**, the respective samples were heated at 140 °C in vacuum overnight. TGA confirmed that there was no further weight loss.

Fluorescence-sensing measurements: The luminescence properties of **Tb_{0.08}Gd_{0.92}L** and **Yb_{0.10}Gd_{0.90}L** were investigated in various solvent emulsions at room temperature. The emulsions were prepared by introducing **Tb_{0.08}Gd_{0.92}L** or **Yb_{0.10}Gd_{0.90}L** (4.00 mg) in powder form into DMF (*N,N*-dimethylformamide), methanol, ethanol, acetone, 1-propanol, 2-propanol, phenylmethanol, toluene, chloroform, acetonitrile, THF (tetrahydrofuran), and H_2O (4.00 mL each). For the experiments on the sensing of solvents, different amounts of acetone were added to a standard emulsion in 2-propanol, while keeping the concentration of the Ln^{3+} ions the same. PL spectra of the emulsions were measured after aging for 3 days and then vigorously agitating with ultrasound. Solvent vapor sensing experiments were performed according to previously reported procedures.^[6c]

Acknowledgements

This work was supported by the National Natural Science Fund of China (21101148, 21171162, 21301168), Jilin Province Youth Foundation (201201005, 20130522132JH, 20130522123JH), the CIAC startup fund, and SRF for ROCS (State Education Ministry).

- [1] a) M. D. Allendorf, C. A. Bauer, R. K. Bhakta, R. J. T. Houka, *Chem. Soc. Rev.* **2009**, *38*, 1330; b) D. MasPOCH, D. Ruiz-Molina, J. Veciana, *Chem. Soc. Rev.* **2007**, *36*, 770; c) J. G. Bünzli, C. Piguet, *Chem. Soc. Rev.* **2005**, *34*, 1048; d) B. V. Harbuzaru, A. Corma, F. Rey, P. Atienzar, J. L. Jord, H. García, D. Ananias, L. D. Carlos, J.

- Rocha, *Angew. Chem.* **2008**, *120*, 1096; *Angew. Chem. Int. Ed.* **2008**, *47*, 1080; e) P. Horcajada, C. Serre, D. Grosso, C. Boissière, S. Perruchas, C. Sanchez, G. Férey, *Adv. Mater.* **2009**, *21*, 1931; f) H. Yang, X. W. He, F. Wang, Y. Kang, J. Zhang, *J. Mater. Chem.* **2012**, *22*, 21849; g) J. Zhang, S. M. Chen, H. Valle, M. Wong, C. Austria, M. Cruz, X. H. Bu, *J. Am. Chem. Soc.* **2007**, *129*, 14168; h) J. Sun, D. Sun, S. Yuan, D. X. Tian, L. L. Zhang, X. P. Wang, D. F. Sun, *Chem. Eur. J.* **2012**, *18*, 16525; i) J. Sun, F. N. Dai, W. B. Yuan, W. H. Bi, X. L. Zhao, W. M. Sun, D. F. Sun, *Angew. Chem.* **2011**, *123*, 7199; *Angew. Chem. Int. Ed.* **2011**, *50*, 7061.
- [2] a) L. D. Carlos, R. A. S. Ferreira, V. de Zea Bermudez, S. J. L. Ribeiro, *Adv. Mater.* **2009**, *21*, 509; b) K. Binnemans, *Chem. Rev.* **2009**, *109*, 4283; c) J. Feng, H. J. Zhang, *Chem. Soc. Rev.* **2013**, *42*, 387; d) K. A. White, D. A. Chengelis, K. A. Gogick, J. Stehman, N. L. Rosi, S. Petoud, *J. Am. Chem. Soc.* **2009**, *131*, 18069; e) S. I. Weissman, *J. Chem. Phys.* **1942**, *10*, 214; f) F. J. Steemers, W. Verboom, D. N. Reinhoudt, E. B. van der Tol, J. W. Verhoeven, *J. Am. Chem. Soc.* **1995**, *117*, 9408.
- [3] a) P. Horcajada, R. Gref, T. Baati, P. K. Allan, C. Serre, *Chem. Rev.* **2012**, *112*, 1232; b) L. E. Kreno, M. Allendorf, J. T. Hupp, *Chem. Rev.* **2012**, *112*, 1105; c) J. G. Bünzli, *Chem. Rev.* **2010**, *110*, 2729; d) K. M. L. Taylor-Pashow, J. D. Rocca, Z. G. Xie, S. Tran, W. B. Lin, *J. Am. Chem. Soc.* **2009**, *131*, 14261; e) K. M. L. Taylor-Pashow, A. Jin, W. B. Lin, *Angew. Chem.* **2008**, *120*, 7836; *Angew. Chem. Int. Ed.* **2008**, *47*, 7722; f) Q. Ju, D. T. Tu, Y. S. Liu, R. F. Li, H. M. Zhu, J. C. Chen, Z. Chen, M. D. Huang, X. Y. Chen, *J. Am. Chem. Soc.* **2012**, *134*, 1323; g) D. T. Tu, Y. S. Liu, H. M. Zhu, R. F. Li, L. Q. Liu, X. Y. Chen, *Angew. Chem.* **2013**, *125*, 1166; *Angew. Chem. Int. Ed.* **2013**, *52*, 1128.
- [4] a) A. P. de Silva, H. Q. N. Gunaratne, T. Gunnlaugsson, A. J. M. Huxley, C. P. McCoy, T. E. Rice, *Chem. Rev.* **1997**, *97*, 1515; b) K. Rurack, U. Resch-Genger, *Chem. Soc. Rev.* **2002**, *31*, 116; c) V. Amendola, L. Fabbri, F. Forti, M. Licchelli, C. Mangano, P. Pallavicini, A. Poggi, D. Sacchi, A. Taglietti, *Coord. Chem. Rev.* **2006**, *250*, 273; d) S. H. Yoon, E. W. Miller, Q. W. He, P. H. Do, C. J. Chang, *Angew. Chem.* **2007**, *119*, 6778; *Angew. Chem. Int. Ed.* **2007**, *46*, 6658; e) K. Hanaoka, K. Kikuchi, H. Kojima, Y. Urano, T. Nagano, *J. Am. Chem. Soc.* **2004**, *126*, 12470.
- [5] a) Y. J. Cui, Y. F. Yue, G. d. Qian, B. L. Chen, *Chem. Rev.* **2012**, *112*, 1126; b) Y. Q. Lan, H. L. Jiang, S. L. Li, Q. Xu, *Inorg. Chem.* **2012**, *51*, 7484; c) B. L. Chen, Y. Yang, F. Zapata, G. N. Lin, G. D. Qian, E. B. Lobkovsky, *Adv. Mater.* **2007**, *19*, 1693; d) F. Y. Yi, W. T. Yang, Z. M. Sun, *J. Mater. Chem.* **2012**, *22*, 23201.
- [6] a) W. S. Liu, T. Q. Jiao, Y. Z. Li, Q. Z. Liu, M. Y. Tan, H. Wang, L. F. Wang, *J. Am. Chem. Soc.* **2004**, *126*, 2280; b) Y. Q. Lan, H. L. Jiang, S. L. Li, Q. Xu, *Adv. Mater.* **2011**, *23*, 5015; c) P. Wang, J. P. Ma, Y. B. Dong, *Chem. Eur. J.* **2009**, *15*, 10432; d) G. S. Yang, Z. L. Lang, H. Y. Zang, Y. Q. Lan, W. W. He, X. L. Zhao, L. K. Yan, X. L. Wang, Z. M. Su, *Chem. Commun.* **2013**, *49*, 1088; e) Y. Li, S. S. Zhang, D. T. Song, *Angew. Chem. Int. Ed.* **2013**, *52*, 710.
- [7] a) S. V. Eliseeva, J. C. G. Bünzli, *Chem. Soc. Rev.* **2010**, *39*, 189; b) K. A. White, D. A. Chengelis, M. Zeller, S. J. Geib, J. Szakos, S. Petoud, N. L. Rosi, *Chem. Commun.* **2009**, 4506; c) L. N. Sun, W. P. Mai, S. Dang, Y. N. Qiu, W. Deng, L. Y. Shi, W. Yan, H. J. Zhang, *J. Mater. Chem.* **2012**, *22*, 5121; d) K. Binnemans, in *Handbook on the Physics and Chemistry of Rare Earths*, Vol. 35 (Eds.: K. A. Gschneidner, Jr., J. C. G. Bünzli, V. K. Pecharsky), Elsevier, Amsterdam, **2005**, Chapter 225, pp. 107.
- [8] a) F. F. Chen, Z. Q. Chen, Z. Q. Bian, C. H. Huang, *Coord. Chem. Rev.* **2010**, *254*, 991; b) M. H. V. Werts, R. H. Woudenberg, P. G. Emmerink, R. Van Gassel, J. W. Hofstraat, J. W. Verhoeven, *Angew. Chem.* **2000**, *112*, 4716; *Angew. Chem. Int. Ed.* **2000**, *39*, 4542; c) L. N. Sun, H. J. Zhang, L. S. Fu, F. Y. Liu, Q. G. Meng, C. Y. Peng, J. B. Yu, *Adv. Funct. Mater.* **2005**, *15*, 1041.
- [9] a) H. Uh, S. Petoud, C. R. Chim. **2010**, *13*, 668; b) J. C. G. Bünzli, G. R. Choppin, in *Lanthanide Probes in Life, Chemical and Earth Sciences - Theory and Practice*, Elsevier, Amsterdam, **1989**.
- [10] Z. Y. Guo, H. Xu, S. Q. Su, J. F. Cai, S. Dang, S. C. Xiang, G. D. Qian, H. J. Zhang, M. O'Keeffe, B. L. Chen, *Chem. Commun.* **2011**, *47*, 5551.
- [11] a) J. Zyss, D. S. Chemia, in *Nonlinear Optical Properties of Organic Molecules and Crystals*, Vol. 1 (Eds.: D. S. Chemia, J. Zyss), Academic Press, Orlando, USA, **1987**, pp. 23; b) J. Zyss, E. Ledoux, *Chem. Rev.* **1994**, *94*, 77; c) F. Auzel, *Chem. Rev.* **2004**, *104*, 139; d) G. L. Law, K. L. Wong, K. K. Lau, S. to Lap, P. A. Tanner, F. Kuo, W. T. Wong, *J. Mater. Chem.* **2010**, *20*, 4074.
- [12] a) D. N. Nikogosian, in *Nonlinear Optical Crystals: A Complete Survey*, Springer-Science, New York, **2005**; b) F. J. Duarte, in *Tunable Laser Applications*, 2nd ed. (Ed.: F. J. Duarte), CRC, New York, **2009**; c) C. Wang, T. Zhang, W. B. Lin, *Chem. Rev.* **2012**, *112*, 1084; d) T. Verbiest, S. V. Elshocht, M. Kauranen, L. Helleman, J. Snauwaert, *Science* **1998**, *282*, 913; e) W. M. Laidlaw, R. G. Denning, T. Verbiest, *Nature* **1993**, *363*, 58; f) A. Rice, Y. Jin, X. F. Ma, X. C. Zhang, D. Bliss, J. Larkin, M. Alexander, *Appl. Phys. Lett.* **1994**, *64*, 1324; g) M. Han, G. Giese, J. F. Bille, *Opt. Express* **2005**, *13*, 5791.
- [13] a) N. Tancrez, C. Feuvrie, I. Ledoux, J. Zyss, L. Toupet, H. Le Bozec, O. Maury, *J. Am. Chem. Soc.* **2005**, *127*, 13474; b) K. L. Wong, G. L. Law, W. M. Kwok, W. T. Wong, D. L. Phillips, *Angew. Chem.* **2005**, *117*, 3502; *Angew. Chem. Int. Ed.* **2005**, *44*, 3436; c) J. M. Shi, W. Xu, Q. Y. Liu, F. L. Liu, Z. L. Huang, H. Lei, W. T. Yu, Q. Fang, *Chem. Commun.* **2002**, 756.
- [14] a) C. Andraudand, O. Maury, *Eur. J. Inorg. Chem.* **2009**, 4357; b) C. M. Liu, J. L. Zuo, D. Q. Zhang, D. B. Zhu, *CrystEngComm* **2008**, *10*, 1674; c) S. Dang, J. H. Zhang, Z. M. Sun, H. J. Zhang, *Chem. Commun.* **2012**, *48*, 11139; d) Q. Ye, Y. H. Li, Q. Wu, H. Zhao, R. G. Xiong, *Chem. Eur. J.* **2005**, *11*, 988; e) M. L. Wei, R. P. Sun, K. Jiang, L. Yang, *J. Coord. Chem.* **2008**, *61*, 3800.
- [15] S. Dang, J. H. Zhang, Z. M. Sun, *J. Mater. Chem.* **2012**, *22*, 8868.
- [16] a) Y. Luo, G. Calvez, S. Freslon, K. Bernot, C. Daiguebonne, O. Guillo, *Eur. J. Inorg. Chem.* **2011**, 3705; b) D. F. Sava, L. E. S. Rohwer, M. A. Rodriguez, T. M. Nenoff, *J. Am. Chem. Soc.* **2012**, *134*, 3983; c) N. Kerbellec, D. Kustaryono, V. Haquin, M. Etienne, C. Daiguebonne, O. Guillo, *Inorg. Chem.* **2009**, *48*, 2837.
- [17] a) D. L. Dexter, *J. Chem. Phys.* **1953**, *21*, 836; b) S. Dang, L. N. Sun, H. J. Zhang, X. M. Guo, Z. F. Li, J. Feng, H. D. Guo, Z. Y. Guo, *J. Phys. Chem. C* **2008**, *112*, 13240.
- [18] a) C. Y. Peng, H. J. Zhang, J. B. Yu, Q. G. Meng, L. S. Fu, H. R. Li, L. N. Sun, X. M. Guo, *J. Phys. Chem. B* **2005**, *109*, 15278; b) P. Wang, R. Q. Fan, X. R. Liu, L. Y. Wang, Y. L. Yang, W. W. Cao, B. Yang, W. Hasi, Q. Su, Y. Mu, *CrystEngComm* **2013**, *15*, 1931; c) I. Oueslati, R. A. S. Ferreira, L. D. Carlos, C. Baleizão, M. N. Berberan-Santos, B. de Castro, J. Vicens, U. Pischel, *Inorg. Chem.* **2006**, *45*, 2652.
- [19] a) J. X. Ma, X. F. Huang, X. Q. Song, W. S. Liu, *Chem. Eur. J.* **2013**, *19*, 3590; b) H. H. Li, W. Shi, K. N. Zhao, Z. Niu, H. M. Li, P. Cheng, *Chem. Eur. J.* **2013**, *19*, 3358; c) C. Y. Sun, X. L. Wang, C. Qin, J. L. Jin, Z. M. Su, P. Huang, K. Z. Shao, *Chem. Eur. J.* **2013**, *19*, 3639.
- [20] a) C. F. Sun, C. L. Hu, X. Xu, B. P. Yang, J. G. Mao, *J. Am. Chem. Soc.* **2011**, *133*, 5561; b) C. F. Sun, C. L. Hu, X. Xu, J. B. Ling, T. Hu, F. Kong, X. F. Long, J. G. Mao, *J. Am. Chem. Soc.* **2009**, *131*, 9486; c) M. C. Chen, L. M. Wu, H. Lin, L. J. Zhou, L. Chen, *J. Am. Chem. Soc.* **2012**, *134*, 6058.

Received: April 10, 2013

Revised: August 23, 2013

Published online: November 6, 2013